Temporal Separation Detection for Chipless Depolarizing Frequency-Coded RFID

Angel Ramos, Etienne Perret, Olivier Rance, Smail Tedjini, Antonio Lazaro, David Girbau

Temporal Separation Detection for Chipless Depolarizing Frequency-Coded RFID

A. Ramos, E. Perret, *Senior Member, IEEE*, O. Rance, *Student Member, IEEE,* S. Tedjini, *Senior Member, IEEE*, A. Lazaro, *Member, IEEE*, and D. Girbau, *Senior Member, IEEE*

***Abstract*—This paper studies the detection of chipless frequency-coded tags. The detection exploits a temporal separation that allows obtaining the identification (ID) with only one measurement. In this way, the flexibility of reading of this type of chipless tags is clearly improved, which is highly expected for future real implementation. This temporal separation is possible when the tag presents a long-time signature, longer than the backscattering wave corresponding to the surrounding objects. A technique based on the short-time Fourier transform is used to differentiate the useful parts of the signal which contain the tag ID. Up to now, this was done by using a calibration process based on two measurements at least to remove coupling and clutter contribution. With the proposed approach the acquisition of the tag ID is direct, and it is not necessary to have further information such as the measurement the environment without the tag. A study on the time duration of several frequency-coded tags is performed based on simulations and measurements. The study shows that this approach can be used with classical depolarizing chipless tags already proposed in the literature. It is proven that the proposed approach is useful to detect the tag response with a single measurement.**

***Index Terms*— Chipless RFID, Radio-frequency Identification (RFID), Ultra-wideband (UWB), time domain, short-time Fourier transform (STFT)**

I. Introduction

Radio frequency identification (RFID) consists of a reader which remotely retrieves information from tags. The tags are attached to objects to be identified. The fact that objects can be considered to be unknown, as well as the fact that the environment can change during the reading, are RFID specific features that require huge considerations, notably during the tag design process [1]. One of the most used technologies is UHF RFID, where each tag has a chip which modulates a narrowband scattering antenna. The cost of each UHF tag is limited mainly by the chip and the process of soldering it on the tag antenna. Recently, there have been several investigations with the aim to remove the chip and reduce tag costs [1]-[5]. This family of tags is known as chipless. Chipless tags consist of permanent physical modifications which modulate the reader signal. Contrary to radar targets, the tag geometry is controlled in order to present a specific and recognizable RF signature. Different chipless RFID tags have been developed recently [1]. Chipless tags operating in the frequency domain are known to be more efficient in terms of coding capacity [6] and, therefore, are investigated in this paper.

Currently, one of main challenges of the chipless technology is the robustness of tag detection in different environments [7]-[9]. It is useless to try to increase the quantity of information that a chipless tag can have if the tag ID cannot be read properly in real environments and without complex calibration techniques. The detection of a chipless tag in noisy environments is much more difficult in chipless RFID than in UHF RFID due to the absence of modulation in time, that is, the absence of two different states in the backscattering signal. Up to now, in chipless, a first measurement of the environment without the tag (background or empty environment) is needed. After that, the ID of the tag is obtained by doing the difference between the background measurement and the measurement with the tag [6]-[7]. This processing is necessary because in chipless RFID the radar cross section (RCS) of tags is very small compared to the RCS of the background [1]. The negligible useful signal of the tag is superposed with an (unknown) background signal, which prevents any reading. In order to read the tag with only one measurement, specific techniques have to be implemented, aiming to separate the contribution of the tag from the contribution of the environment. Detection of chipless RFID tags using time-domain approaches has been proposed recently. In [4] a detection technique based on the continuous Wavelet transform is used to detect time-coded chipless tags. Time-frequency approaches to detect frequency signatures of chipless RFID tags have been studied recently. In [10], a time-windowing technique is used in frequency-coded tags (tags based on two antennas in cross polarization, connected by a transmission line loaded with dual-band resonators). A similar approach is used in [11] to detect the response of a wireless sensor. In [12], a 3-bit chipless RFID frequency-coded tag is detected using the short-time matrix pencil method (STMPM). This method uses the imaginary parts of the poles of the

Manuscript received February 4, 2015. This work was supported by the Spanish Government Project TEC2011-28357-C02-01, the AGAUR Grant FI-DGR 2012 and the European Commission RISE Project 645771 "ChiplEss MultisEnsor Rfid for GrEen NeTworks (EMERGENT)". A. Ramos, A. Lazaro and D. Girbau are with the Department of Electronic, Electrical and Automatic Control Engineering, Universitat Rovira i Virgili, 43007 Tarragona, Spain (angel.ramos@urv.cat, antonioramon.lazaro@urv.cat, david.girbau@urv.cat). E. Perret, O. Rance and S. Tedjini are with the Laboratoire de Conception et d'Intégration des Systèmes (LCIS) / Grenoble Institute of Technology, Valence 26000, France (etienne.perret@lcis.grenoble-inp.fr, olivier.rance@lcis.grenoble-inp.fr, smail.tedjini@lcis.grenoble-inp.fr). E. Perret is also with the Institut Universitaire de France (IUF).

STMPM, and is able to detect the resonances associated tag in front of noise. The same authors propose a technique to design improved 24-bit tags in [13]. In both cases, measurements at a tag-reader distance of 50 cm in co-polarization are provided. Also, besides the tag measurement, two more measurements are required to calibrate the system. Finally, in [14], the same STMPM technique is proposed and compared with other time-frequency techniques to study the behavior of resonant structures. Simulations of dipoles and a circular cavity in co-polarization are provided.

Recently, in [7] a significant improvement in terms of chipless tag robustness of detection has been obtained. Based on the "RF encoding particles" approach, hereafter referred to as REP and a depolarization technique, it has been shown that a REP tag can be read whatever the object on which the tag is placed. This means that in addition to the tag measurement, only one other measurement is needed. This second measurement is done without the tag but also without the object where the tag is attached. Therefore, the object does not have to be known, and the tag can be read at different positions in a 3D area (within its read range).

Based on a time-frequency point of view, [10], [13], this work proposes a time separation approach to improve considerably the detection of chipless depolarizing RFID tags [7]. It is studied how the time duration of the tag can be exploited to separate the tag contribution from the tag's environment. To this end, different tag structures (depolarizing and non-depolarizing) are compared theoretically and by simulations and measurements. Then, the Short-Time Fourier Transform (STFT) is used [15] to effectively separate the different contributions. The STFT is a well-known technique for audio and speech processing, which has been also studied for chipless RFID [16].

By combining the STFT with robust depolarizing tags [7], the tag response can be obtained without any calibration measurement. This is possible because frequency domain depolarizing chipless tags are intrinsically resonant structures, designed to have high quality factor in order to present a high radar cross section (RCS). It is why their quality factor is higher than the one coming from the surrounding objects. So the tags will store energy corresponding to their frequency of resonances, and by suppressing the early-time scattering, tag identification based on the late-time signal part could be possible [17]. The discrimination based on this ascertainment will be shown for several chipless resonant tag structures.

The paper is organized as follows. Section II presents the theory and the measurement setup of frequency-coded depolarizing chipless RFID tags. Then, the Short-Time Fourier transform is presented as a technique to detect tags with high quality factors in real environment with a single measurement. Section III studies the quality factor of several tags, based on simulations. Section IV presents the experimental results with depolarizing tags. Finally, Section V draws the conclusions.

II. THEORY

A. Time Separation with Depolarizing Frequency-Coded Chipless RFID

Fig. 1a shows a scheme of the depolarizing chipless RFID system along with the signals involved. The reader transmits a wideband horizontally-polarized signal which hits the tag. The tag vertically-polarized backscattered signal part is then received at the reader. The ID is coded in the presence or absence of resonances. The tags are composed by REPs, which act as a transmitting/receiving antenna and a filtering circuit. In [7], a block diagram of the channel model was developed to illustrate linear and systematic errors arising in a polarimetric measurement. It was shown that for cross-polarization measurements, the majority of the error terms could be neglected, leading to a simple expression for the signal at the reader. A new version of the block diagram is proposed in Fig. 1b to emphasize the time-dependence of the model. Symbols $a_{\mathrm{h,v}}$ and $b_{\mathrm{h,v}}$ denote the transmitted and received power waves in horizontal (h) and vertical (v) polarizations, respectively. Symbols $E^{t,r}$ denote the transmitted and received electric field, respectively. Symbols $E^{i,s}$ denote the incoming and backscattered field at the tag. β is the phase constant, d is the distance between reader's antennas, and R is the distance between the reader's antennas and the tag. Compared to the diagram proposed in [7], the delays due to propagation in free space are now shown explicitly. Following the same derivation than in [7] gives:

$$M_{vh} = I_{vh}e^{-j\beta d} + R_{vv}C_{vh}T_{hh}e^{-2j\beta R} + R_{vv}O_{vh}T_{hh}e^{-2j\beta R_0}\,, \qquad (1)$$

where I_{vh} is the direct coupling from the reader's transmitting to receiving antenna in cross-polarization. R_{vv} is the receive path in vertical polarization, T_{hh} is the transmitted path in horizontal polarization, C_{vh} is the scattering matrix corresponding to tag response in cross-polarization, and O_{vh} is the response of the surrounding object in cross-polarization. As for common objects O_{vh} is generally negligible, this type of tag and configuration has proven to be robust in front of surrounding objects near the tag [7]. The tag ID is obtained by subtracting the measurements of tags M_{vh} from the empty measurement I_{vh}. It is important to notice that, in such a case, a calibration procedure using a reference object is not necessary to find the ID of the tag. Indeed, even if the coefficients R_{vv} and T_{hh} are not known (the distortion introduced is low enough so the peaks in frequency who encode the data are still recognizable), the tag ID can be deduced form $R_{vv}C_{vh}T_{hh}$ which simply corresponds to M_{vh} - I_{vh}. But I_{vh} is needed, that means that two measurements must be done. Even though the coupling I_{vh}, is cross-polarized, its power is strong enough (because of the proximity between the reader's antennas) to prevent any reading. By using a simplified model for the time domain behavior of each block, a simple approximate equation of the whole system can be obtained:

$$
\begin{aligned}
&s(t) = m_{vh}(t) * p(t) = \\
&= i_{vh}(t) + c_{vh,s}(t) + c_{vh,a}(t) + o_{vh}(t) = \\
&A_1 \frac{d^2 p}{dt^2}(t-\tau_d) \\
&+A_2 \frac{d^2 p}{dt^2}(t-2\tau_R) \\
&+A_3 \cdot u(t-2\tau_R) e^{-\frac{\omega_0 (t-2\tau_R)}{2Q}} \cos\left(\omega_0 (t-2\tau_R)\right) \\
&+A_4 \frac{d^2 p}{dt^2}(t-2\tau_{R_0})
\end{aligned}
\quad , \qquad (2)
$$

where $p(t)$ is the emitted pulse, A_1, A_2, A_3, and A_4 are proportionality constants determining the amplitude of the different components, u is the unit step function , ω_0 is the angular frequency, Q is the quality factor and τ_d, τ_R and τ_{R0} are the delays due to free space propagation on the corresponding distances. The transmitting and receiving paths (T, R in Fig. 1b) are dominated by the antennas effect. It is well known from UWB radar theory that if the target is in the farfield of the antennas, each antenna acts as a time-derivative of the signal. The first term in the summation corresponds to the direct coupling ($I_{vh}e^{-j\beta d}$), A_1 can be seen as the transmission coefficient between antennas. The second derivative of the pulse is due to antennas effects. The second and the third terms are corresponding to the response of the tag ($R_{vv}C_{vh}T_{hh}e^{-2j\beta R}$). The tag response has been separated into two components to clearly distinguish the early time (structural mode) from the late time (antenna mode). The early time corresponds approximately to a specular reflection of the pulse and A_2 can be seen as a reflection coefficient. During the early time, part of the incident energy is coupled to the tag. After extinction of the pulse (late time), the tag shows free damped oscillations which do not depend on the pulse shape anymore. A_3 accounts for the coupling coefficient as well as antennas effects. The step function is necessary to ensure causality. The fourth term corresponds to the response of the object ($R_{vv}O_{vh}T_{hh}e^{-2j\beta R_0}$) which is considered not resonant. It can be approximated by a specular reflection with A_4 corresponding to the reflection coefficient. As before, second derivative of the pulse is due to antennas.

Fig. 1c shows a scheme of the signals in detail in time domain. As it can be observed, objects near the tag, although they do not depolarize the incoming signal (and should have small amplitude in reception), can distort the tag response. By gating in time-domain the undesired contributions, i.e., $i_{vh}(t)$ and $o_{vh}(t)$, the resonances can be detected in front of these induced perturbations. The signal corresponding to the signal at the reader in co-polarization is also shown. Time constants τ_I, τ_C can be associated to the time response (or time duration) of $i_{vh}(t)$ and $c_{vh,a}(t)$, respectively. Similarly, and as an example for two nearby objects, τ_{O1} and τ_{O2} can be associated to $o_{vh}(t)$. If τ_I, τ_{O1}, $\tau_{O2} << \tau_C$, that is, the time duration of the tag is longer than the time response of the coupling and nearby objects, these signals can be separated, and for $t >> \tau_{O2}$ (τ_{O2} is the time constant of the object that is more away from the tag):

$$
m_{vh}(t) * p(t) \approx c_{vh,a}(t) \, . \qquad (3)
$$

Therefore, by using the late-time part of signal, we will see that it is possible with one measurement $c_{vh,a}$ to extract the tag ID.

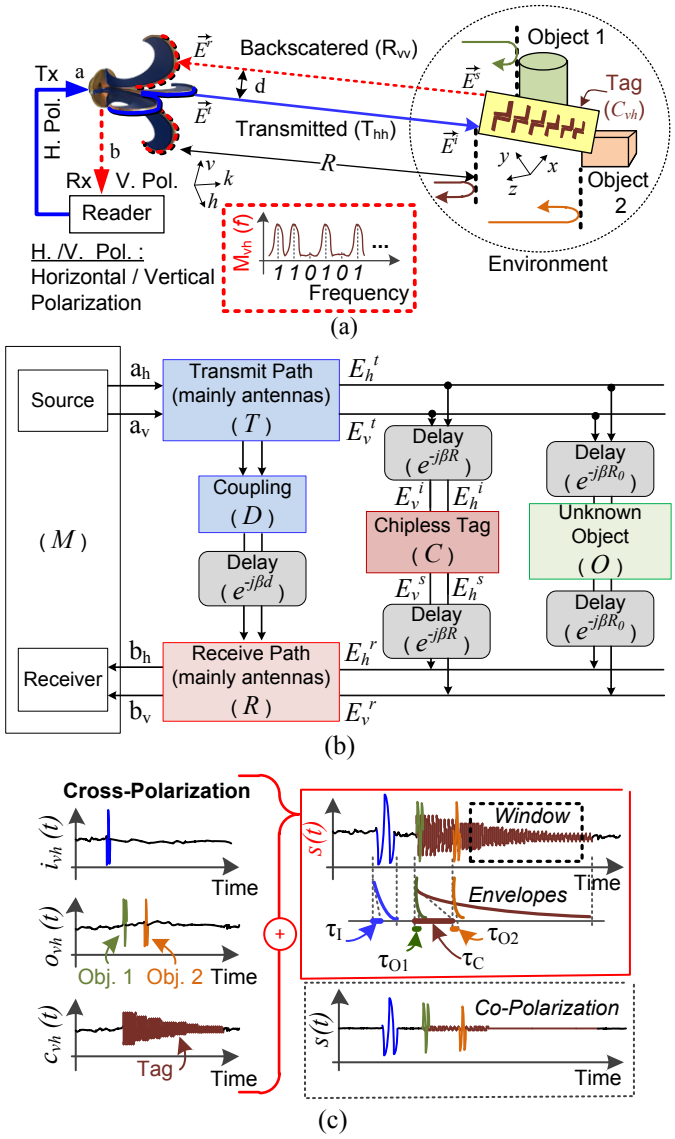

Fig. 1. (a) Scheme of the depolarizing chipless RFID system and the tag identification signal in frequency domain. (b) Channel model of the system, accounting for the propagation delays. (c) Scheme of the signals in time domain.

B. *Short-Time Fourier Transform*

The Short-Time Fourier Transform of a given signal $s(t)$ can be defined as [15], [18]:

$$
S(\omega,\tau) = \int_{-\infty}^{+\infty} s(t) w(\tau - t) e^{-j\omega t} dt \, , \qquad (4)
$$

where $\omega = 2\pi f$ is the angular frequency and τ is the time across $w(t)$ is shifted. $w(t)$ is a weighting function or time window,

i.e., the impulse response of a lowpass filter. It is desired that *w(t)* has a finite impulse response (FIR), or duration in time.

The STFT can be seen as the Fourier transform of a time weighted signal, where τ is the time where the weighting function *w(t)* is centered. This transform can also be seen as the output of a complex baseband filter bank. As explained in Section II.A, frequency-coded chipless tags rely on the presence or absence of resonances (peaks) within a wide band. In this case, ω is the center frequency of each bandpass filter and τ is the time when the filter output is sampled. In order to derive the filter bank interpretation, the impulse response of the bandpass filter can be expressed as:

$$h_\omega(t) = w(t)e^{j\omega t}. \tag{5}$$

Then, (4) can be expressed as:

$$\begin{aligned} S(\omega,\tau) &= w(t) * \left[e^{j\omega t} s(t) \right] = e^{-j\omega\tau} \int s(t) w(\tau - t) e^{-j\omega(t-\tau)} dt \\ &= e^{-j\omega\tau} \left[h_\omega(t) * s(t) \right]. \end{aligned} \tag{6}$$

Therefore, the STFT can be seen as the demodulated (by $e^{-j\omega\tau}$) bandpass filtered signal from *s(t)*. Since *w(t)* is lowpass, *S(ω,τ)* is a lowpass function of τ. Then, for each ω, *S* can be sampled at a rate determined by twice the lowpass cutoff frequency (f_c) of the window *w(t)* (from Nyquist's Theorem).

The window *w(t)* plays the most important role in the STFT, since there is a tradeoff between time-limiting and bandwidth-limiting. Concerning frequency-coded tags, a time-limited signal can separate better the coupling and clutter contributions from the actual tag response. However, in this case the frequency peaks associated to the tag ID are wider and difficult to separate. On the contrary, a bandwidth-limited window can provide sharp tag ID peaks, at the cost of including more unwanted signal contributions inside the window [14]. Three typically-used windows are considered to detect the tags: Hamming, Chebyschev and Kaiser [19]. A Hamming window is chosen as a tradeoff solution to have enough resolution both in time and frequency domain. Other windows can be chosen depending on the application [16].

Choosing a correct window length is as important as the shape [16]. Fig. 2 shows a scheme (from an actual measurement) of the time-domain response of a chipless RFID tag, with and without background subtraction. The window *w(t)* is also shown. As observed, coupling (I_{vh}, as detailed in Section II.A) and clutter contributions appear. If a very long window is chosen more noise is captured inside the window, reducing the SNR. If the window length *T* is very long, coupling and objects contribution could be inside of the window for any τ. It is also important to note that, even though it requires more processing time, window overlapping is also used in order to avoid data loss near the window boundaries [19]. Window overlapping consists of choosing small increments of τ ($\tau << T$) in the algorithm.

Using the last two summands of eq. (2), the time and frequency domain response of an ideal resonator interfered by a non-resonant object is calculated. The parameters chosen are: $A_3 = A_4 = 1$ (resonator and interferer have the same amplitude), $\tau_R = 0$, $f_0 = 4$ GHz $Q = 55$, and p corresponding to the absolute value of a second order resonator, that is, $p(t) = 1\Big/\sqrt{1+Q'^2\left(\frac{t}{t_0}-\frac{t_0}{t}\right)^2}$ with $t_0 = 10$ ns and $Q' = 40$. A time window $T = 4$ ns is used. It is important to stress that the object has the same amplitude than the resonator to clearly show both of them. In a real case, the object component would be in cross polarization and, thus, much lower. As it can be observed in Figs. 2b-c, the tag and the object can be detected with the STFT representation. Later in Section IV it will be studied with real measurements.

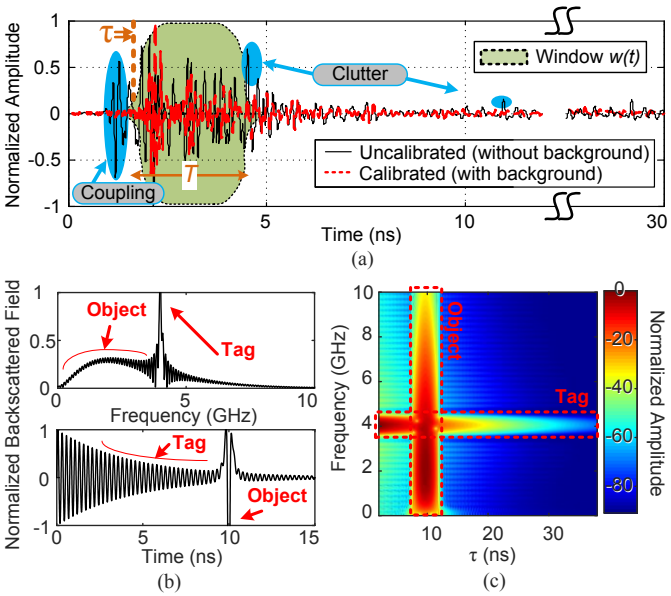

Fig. 2. (a) Scheme of the time-domain response for a frequency-coded chipless RFID tag. (b) Frequency and time signals and corresponding (c) STFT spectrogram representation of a theoretical 4 GHz resonator and a non-resonant object, both with the same amplitude.

REFERENCES

[1] E. Perret, "Radio Frequency Identification and Sensors: From RFID to Chipless RFID," *Wiley-ISTE*, 2014.

[2] S. Preradovic, I. Balbin, N. Chandra Karmakar, and G. F. Swiegers, "Multiresonator-Based Chipless RFID System for Low-Cost Item Tracking," *IEEE Transactions on Microwave Theory and Techniques*, Vol. 57, No. 5, pp. 1411-1419, May 2009.

[3] A. Vena, E. Perret, and S. Tedjini, "Chipless RFID Tag Using Hybrid Coding Technique," *IEEE Transactions on Microwave Theory and Techniques*, Vol. 59, No. 12, pp. 3356-3364, Dec. 2011.

[4] A. Lazaro, A. Ramos, D. Girbau, and R. Villarino, "Chipless UWB RFID Tag Detection Using Continuous Wavelet Transform," *IEEE Antennas and Wireless Propagation Letters*, Vol. 10, pp. 520-523, 2011.

[5] S. Tedjini, N. Karmakar, E. Perret, A. Vena, R. Koswatta, and R. E-Azim, "Hold the Chips: Chipless Technology, an Alternative Technique for RFID," *IEEE Microwave Magazine,* Vol. 14, pp. 56-65, July 2013.

[6] A. Vena, E. Perret, and S. Tedjini, "Design of Compact and Auto Compensated Single Layer Chipless RFID Tag," *IEEE Transactions on Microwave Theory and Techniques,* Vol. 60, pp. 2913 – 2924, September 2012.

[7] A. Vena, E. Perret, and S. Tedjini, "A Depolarizing Chipless RFID Tag for Robust Detection and Its FCC Compliant UWB Reading System,"

IEEE Transactions on Microwave Theory and Techniques, Vol. 61, No. 8, pp. 2982-2994, Aug. 2013.

[8] A. Vena, E. Perret, B. Sorli, and S. Tedjini, "Study on the detection reliability of chipless RFID systems," in *2014 XXXIth URSI General Assembly and Scientific Symposium (URSI GASS)*, Beijing, China, 2014.

[9] T. Andriamiharivolamena, A. Vena, E. Perret, P. Lemaitre-Auger, and S. Tedjini, "Chipless identification applied to human body," in *RFID Technology and Applications Conference (RFID-TA), 2014 IEEE*, 2014, pp. 241-245.

[10] D. Girbau, J. Lorenzo, A. Lazaro, C. Ferrater, and R. Villarino, "Frequency-coded chipless RFID tag based on dual-band resonators," *IEEE Antennas and Wireless Propagation Letters*, Vol. 11, pp. 126-128, 2012.

[11] H. Cheng, S. Ebadi, and X. Gong, "A Low-Profile Wireless Passive Temperature Sensor Using Resonator/Antenna Integration Up to 1000 ºC," *IEEE Antennas and Wireless Propagation Letters*, Vol. 11, pp. 369-372, 2012.

[12] R. Rezaiesarlak and M. Manteghi, "Short-Time Matrix Pencil Method for Chipless RFID Detection Applications," *IEEE Transactions on Antennas and Propagation*, Vol. 61, No. 5, pp. 2801-2806, May 2013.

[13] R. Rezaiesarlak and M. Manteghi, "Complex-Natural-Resonance-Based Design of Chipless RFID Tag for High-Density Data," *IEEE Transactions on Antennas and Propagation*, Vol. 62, No. 2, pp. 899-904, Feb. 2014.

[14] R. Rezaiesarlak and M. Manteghi, "On the Application of Short-Time Matrix Pencil Method for Wideband Scattering From Resonant Structures," *IEEE Transactions on Antennas and Propagation*, Vol. 63, No. 1, pp. 328-335, Jan. 2015.

[15] J. B. Allen, "Applications of the Short Time Fourier Transform to Speech Processing and Spectral Analysis," *7th IEEE International Conf. on Acoustics, Speech, and Signal Processing*, pp. 1012-1015, 1982.

[16] R. Rezaiesarlak and M. Manteghi, "Chipless RFID: Design Procedure and Detection Techniques," *Springer*, 2015.

[17] C. E. Baum, J. E. Rothwell, Y. F. Chen, and D. P. Nyquist "The Singularity Expansion Method and Its Application to Target Identification," *Proceedings of the IEEE*, Vol. 79, No. 10, pp. 1481-1492, Oct. 1991.

[18] K. Grochenig, "Foundations of Time-Frequency Analysis," *Birkhauser Basel - Springer Books*, 2001.

[19] F. J. Harris, "On the Use of Windows for Harmonic Analysis with Discrete Fourier Transform," *Proceedings of the IEEE*, Vol. 66, No. 1, Jan. 1978.

[20] M. Salehi and M. Manteghi, "Transient Characteristics of Small Antennas," *IEEE Transactions on Antennas and Propagation*, Vol. 62, No. 5, pp. 2418-2429, Feb. 2014.

[21] R. E. Collin, "Foundations for Microwave Engineering," *Wiley-Interscience*, 2001.